# Modeling of Turn-on Delay Time Jitter in Vertical-Cavity Surface-Emitting Lasers

Guoying Ding, S. W. Corzine, M. R. T. Tan, S. Y. Wang

The pattern-dependent behavior of the turn-on delay in proton-implanted Vertical-Cavity Surface-Emitting Lasers is modeled with rate equations that include a second carrier reservoir to account for the current spreading underneath the proton-implanted regions. We find that under certain conditions, the carrier density in these regions can increase the turn-on jitter significantly.

Vertical-Cavity Surface-Emitting Lasers (VCSELs) have many advantages over traditional edge-emitting lasers, such as low cost manufacturing, high yield, good beam quality, and scaleable geometries. These properties make VCSELs desirable for many applications. Multimode fiber data links using VCSELs have been successfully demonstrated. [1] Under high bit rate modulation, the turn-on jitter (variation in turn-on delay time) can impose a serious limit on the maximum bit rate that can be achieved.[2-4] While there are studies on this issue for edge-emitting lasers, there have been no studies on VCSELs. In this paper, we report a theoretical study of the pattern-dependence of the turn-on delay time and the effect of carrier diffusion on turn-on jitter for a single-mode proton-implanted VCSEL.

Simulations of the turn-on process are based on a set of single mode rate equations, similar to most standard carrier and photon rate equations.[5] The difference is that we include two carrier components in our model, one is the carriers in the active region which generate stimulated photon emission once the carrier density approaches threshold, like in the standard rate equations; while the other component is a carrier reservoir underneath the proton-implanted regio which does not contribute to stimulated photon emission. The reason this carrier reservoir is incorporated is that in proton-implanted VCSELs, part of the injection current spreads underneath the proton-implanted regions, as the implantation cannot provide perfect isolation. The rate equations are as follows:

$$\frac{dN_1}{dt} = (1-\alpha)\eta\frac{I}{qV_1} - (R_{sp1} + R_{nr1}) - v_g g N_p - \frac{N_1 - N_2}{\tau_d},$$

$$\frac{dN_p}{dt} = (\Gamma v_g g - \frac{1}{\tau_p})N_p + \Gamma R'_{sp},$$

$$\frac{dN_2}{dt} = \alpha\eta\frac{I}{qV_2} - (R_{sp2} + R_{nr2}) + \frac{V_1}{V_2}\frac{N_1 - N_2}{\tau_d}.$$

In these equations, $N_1$ and $N_2$ are the carrier densities in the active region and under the proton-implanted regions, respectively, $V_1$ and $V_2$ are the corresponding volumes of the two regions, $\alpha$ is the percentage of injection current, $I$, going into the second outer carrier reservoir such that $V_2 = \alpha V_1/(1-\alpha)$, $N_p$ is the average photon density, $\tau_p$ is the photon lifetime, $g$ is the material gain, $v_g$ is the group velocity, $\Gamma$ is the three-dimensional confinement factor including standing wave enhancements, $\eta$ is the perpendicular injection efficiency (assumed equal in both reservoirs), $R_{sp}$ is the spontaneous emission rate, $R_{nr}$ is the nonradiative recombination rate including Auger recombination, and $R'_{sp}$ is the spontaneous emission rate into the lasing mode. The coupling term between the two carrier reservoirs includes a *diffusion time*, $\tau_d$, which characterizes the rate of diffusion from one reservoir to the other. It can be expressed as $\tau_d = L^2/2D_{np}$, where $D_{np}$ is the ambipolar diffusion constant and $L$ is some characteristic diffusion length between the two reservoirs. $\tau_d$ is typically in the few nanosecond range but an exact calculation would have to include the spatial dependencies of both carrier and photon densities. Here we use $\tau_d$ as a fitting parameter to observe the basic effects of carrier diffusion between the reservoirs. Typical rate equation parameters appropriate for VCSELs and the dependencies of gain and recombination times on carrier density are taken from Ref. 5 for the following simulations.

The pattern-dependence of the turn-on delay time under pseudo-random bit sequence modulation can be explained by Fig. 1a. In Fig. 1a, the time dependence of the carrier density and photon density are plotted during the turn-on process of two extreme cases: one is with a long string of 0s before switching to 1, the other is with a long string of 1s followed by a single 0 bit before switching back to 1. In the first case, during the long string of 0s, carriers have a long time to decay to a low value before switching to 1, so the time needed for the carrier density to reach the threshold value is large, resulting in a long turn-on delay time. For the second case, since the carriers have only one 0 bit length of time to decay before switching to 1, the carrier density right before the turn-on occurs is higher. Therefore it takes less time for the carrier density to reach the threshold value, and thus the turn-on delay is shorter. This results in a variation of the turn-on delay time depending on the bit pattern of the driving current. An example of the turn-on behavior of carrier and photon densities under pseudo-random word modulation is shown in Fig. 1b. Each trace represents a certain number of 0s before switching to 1. The difference between the maximum and minimum turn-on delay is defined as jitter spread. This characteristic can be observed from both the modified rate equation model with carrier diffusion and the standard rate equations.

The effect of carrier diffusion on jitter spread is shown in Fig. 2. The set of curves are jitter spread vs. diffusion time between the two carrier reservoirs with a different percentage of injection current going into the outer reservoir underneath the proton implanted regions. When more injection current leaks into the outer reservoir, the jitter spread increases. We also see that for a certain range of diffusion times between the two reservoirs, the jitter spread is enhanced dramatically by more than a factor of two. Physically this occurs because the carriers underneath the implanted regions can build up well beyond the threshold level since they do not clamp like the carriers in the active region at threshold. As a result, when the current is turned off, these carriers can act as a temporary supply of carriers which can diffuse into the active region and maintain a higher-than-normal carrier density there for a short time. For the extreme case of only one 0 bit, this translates into shorter-than-normal turn-on times which increases the jitter spread accordingly (the other extreme case of a long string of 0s before turning on is relatively unaffected by the second carrier reservoir since both reservoirs have had time to relax to their steady-state low values).

Note also from Fig. 2 that when the diffusion time is very small or very large, the jitter spread reduces to the single carrier reservoir limit. This is because when $\tau_d$ is very small, there is fast diffusion between the two carrier reservoirs, resulting in a synchronization of the two carrier density levels, making this case essentially equivalent to having no second carrier reservoir. While when the diffusion time is very large, the diffusion between the two is so slow that the second reservoir cannot supply carriers quick enough to the active region after turn-off, and hence it has little effect on the carrier density in the active region. Therefore, for either very small or very large $\tau_d$, the carrier reservoir underneath the implanted region does not increase the jitter spread. The biggest effect occurs when $\tau_d$ is comparable to the carrier lifetime.

Figure 3 shows the relationship between the jitter spread and the modulation bit rate. The upper curve is calculated from the modified rate equations including carrier diffusion while the lower curve is calculated from the standard rate equation model. Jitter spread increases as the bit rate goes higher because as the bit length decreases, the carrier density has less time to relax in one 0 bit time span. This results in a shorter turn-on delay for the extreme case of only one 0 bit, which increases the jitter spread. The amount of jitter spread calculated including the carrier diffusion term is about two times larger than that without this term for the parameters chosen, indicating that the existence of the second carrier reservoir can, under certain conditions, severely degrade the device performance, especially at high speed modulation. Figure 4 shows how the biasing level of the logic 0 can influence the jitter spread. Clearly, if the device is biased above threshold, the jitter

spread is greatly reduced since the carrier density is already at the threshold value. However, the extinction ratio (high-to-low power ratio) is reduced in this case which is undesirable for many applications. Choosing a bias level which reduces the jitter spread without sacrificing the extinction ratio can improve the overall performance considerably.

In conclusion, we have examined the pattern-dependence of the turn-on delay in VCSELs including the existence of carriers underneath the proton implanted regions. Our modified rate equation model which includes two carrier reservoirs and a diffusion term between them indicates that the existence of these perimeter carriers can significantly enhance the jitter spread. The jitter spread also increases with modulation rate but can be minimized by biasing the device near or above threshold.

The authors would like to acknowledge useful discussions with Ian White and Huw Summers.

Guoying Ding ( 226 McCullough, Solid State Electronics Laboratory, Department of Electrical Engineering, Stanford University, Stanford, CA 94305, USA)
S. W. Corzine, M. R. T. Tan, and S. Y. Wang (Hewlett-Packard Laboratories, Palo Alto, CA 94304-1392, USA)

References

[1] K.H. Hahn, M.R. Tan, and S.Y. Wang, “Modal and intensity noise of large-area multiple-transverse-mode VCSELs in multimode-optical-fiber links,” 1994 Conference on Optical Fiber Communication - paper ThB3, OFC ’94.

[2] C.R. Mirasso, P. Colet, and M. San Miguel, “Dependence of timing jitter on bias level for single-mode semiconductor lasers under high speed operation,” *IEEE J. Quantum Electron.*, **QE-29,** pp. 23-32, 1993.

[3] A. Sapia, P. Spano, C.R. Mirasso, P. Colet, and M. San Miguel, “Pattern effects in timing jitter of semiconductor lasers,” *Appl. Phys. Lett.*, **61**, pp. 1748-1750, 1992.

[4] T.-M. Shen, “Timing jitter in semiconductor lasers under pseudorandom word modulation,” *J. Lightwave Technology*, **7**, pp. 1394-1399, 1989.

[5] L.A. Coldren and S.W. Corzine, “Diode Lasers and Photonic Integrated Circuits,” Chapter 5, Wiley Interscience, New York, 1995.

Fig. 1. Switching behavior of carrier and photon densities (bit length = 1 ns): (a) with two different kinds of previous bit patterns before the switching, and (b) under pseudo-random bit sequence modulation.

Fig. 2. Jitter spread vs. diffusion time with different percentages of current going into the outer reservoir.

Fig. 3. Comparison of jitter spread with and without carrier diffusion vs. bit rate assuming $\tau_d = 1\,\text{ns}$ and $\alpha = 40\%$.

Fig. 4. Influence of logic 0 bias on jitter spread assuming $\tau_d = 1\,\text{ns}$ and $\alpha = 40\%$.

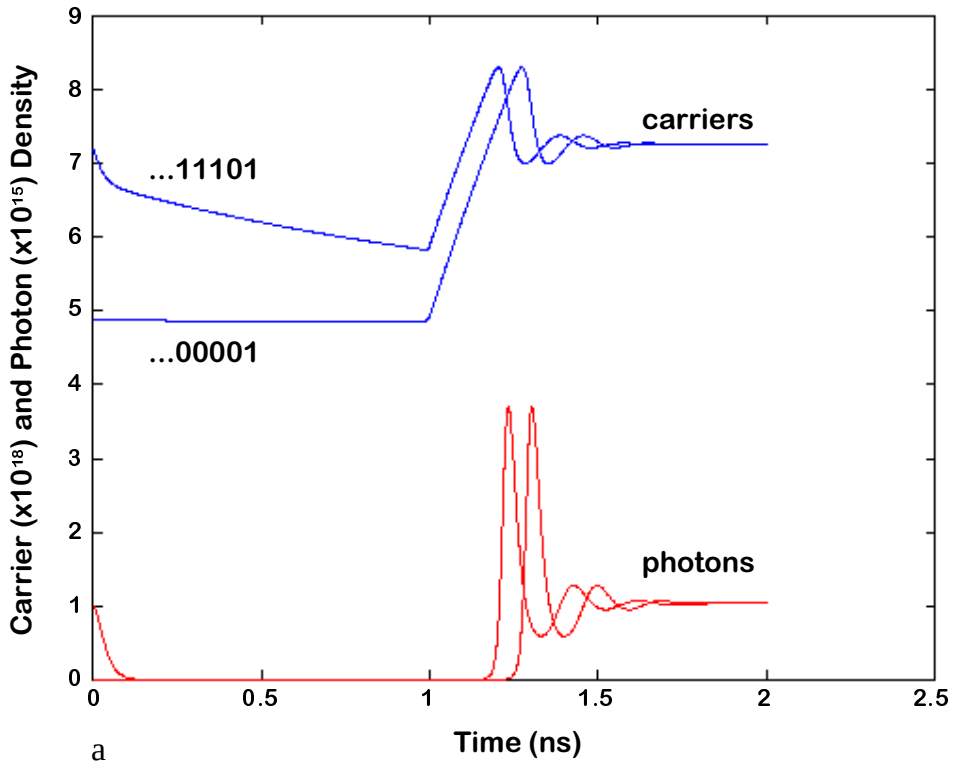


$I_{max} = 5I_{th}$

$I_{min} = 0.5I_{th}$

a

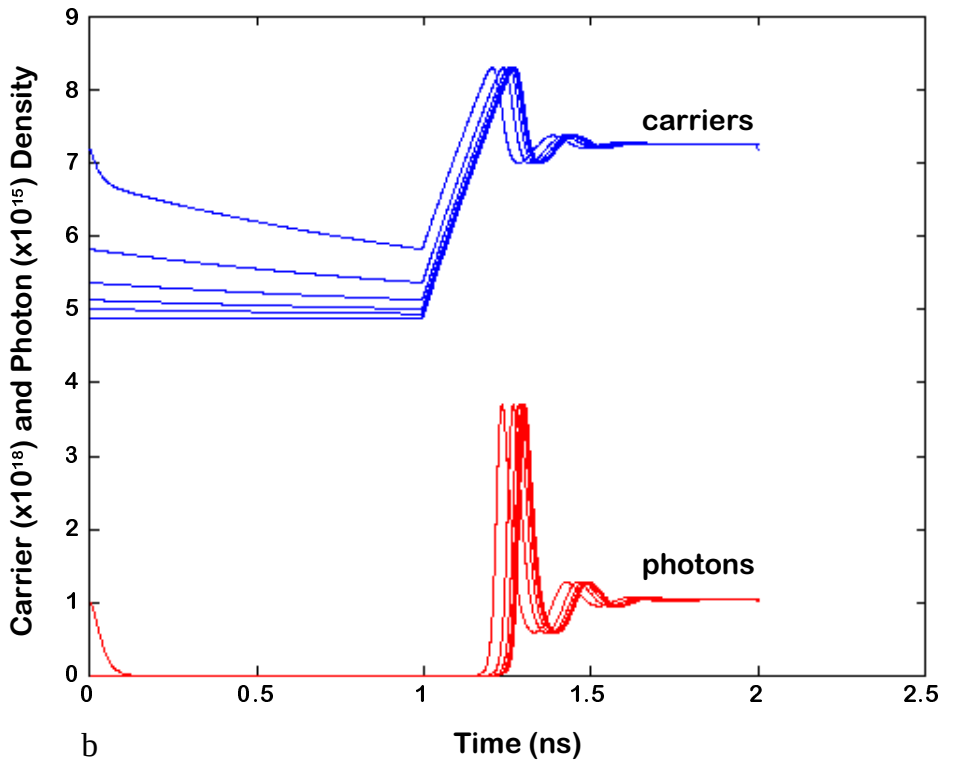


$I_{max} = 5I_{th}$

$I_{min} = 0.5I_{th}$

b

Fig. 1

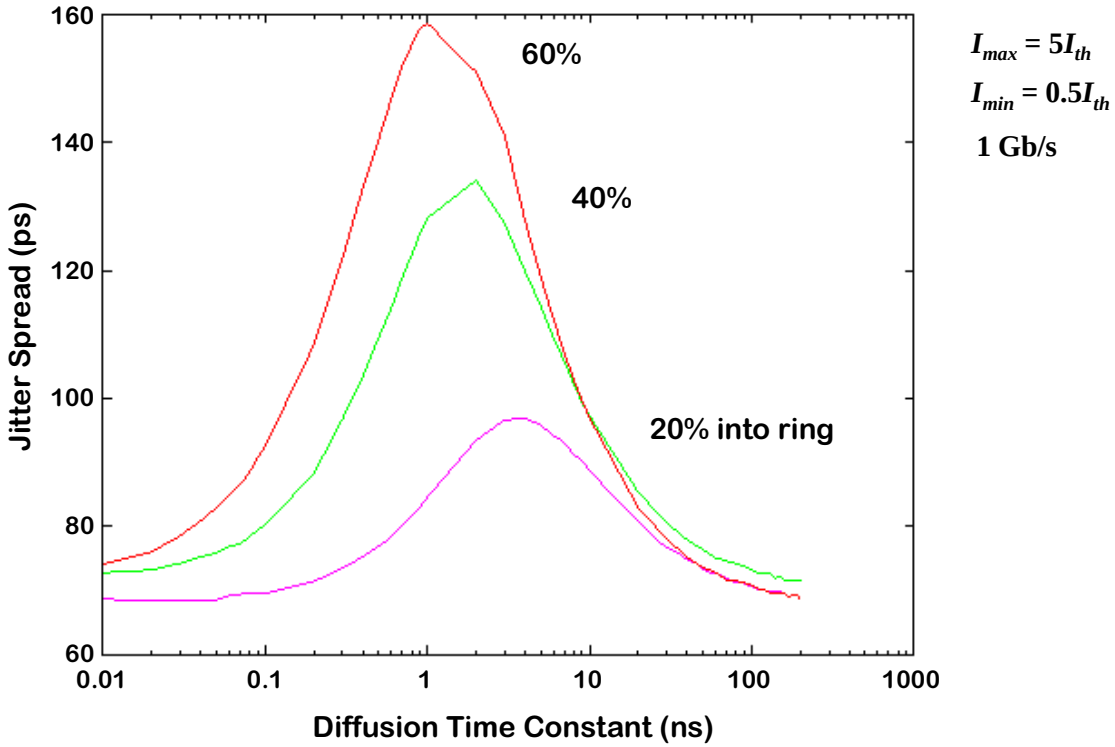
160
140
120
100
80
60
Jitter Spread (ps)
0.01
0.1
1
10
100
1000
Diffusion Time Constant (ns)
60%
40%
20% into ring
$I_{max} = 5I_{th}$
$I_{min} = 0.5I_{th}$
1 Gb/s

Fig. 2

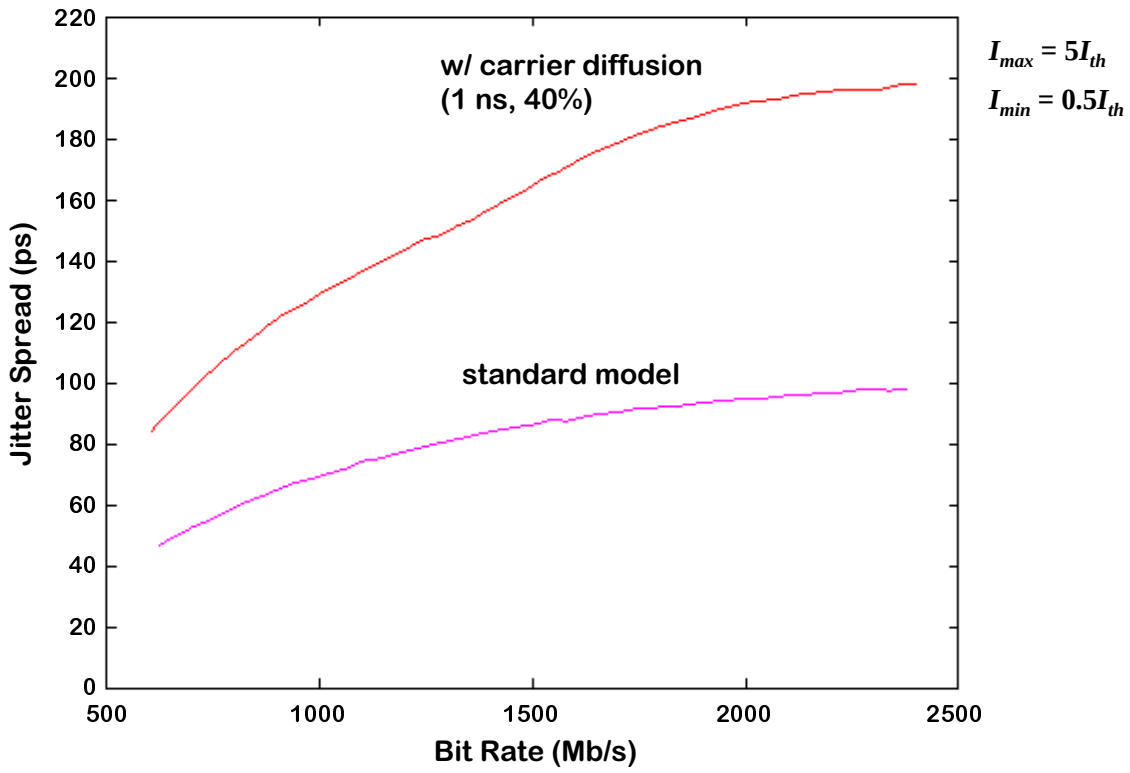
w/ carrier diffusion
(1 ns, 40%)
standard model
Jitter Spread (ps)
Bit Rate (Mb/s)
220
200
180
160
140
120
100
80
60
40
20
0
500
1000
1500
2000
2500
$I_{max} = 5I_{th}$
$I_{min} = 0.5I_{th}$

Fig. 3

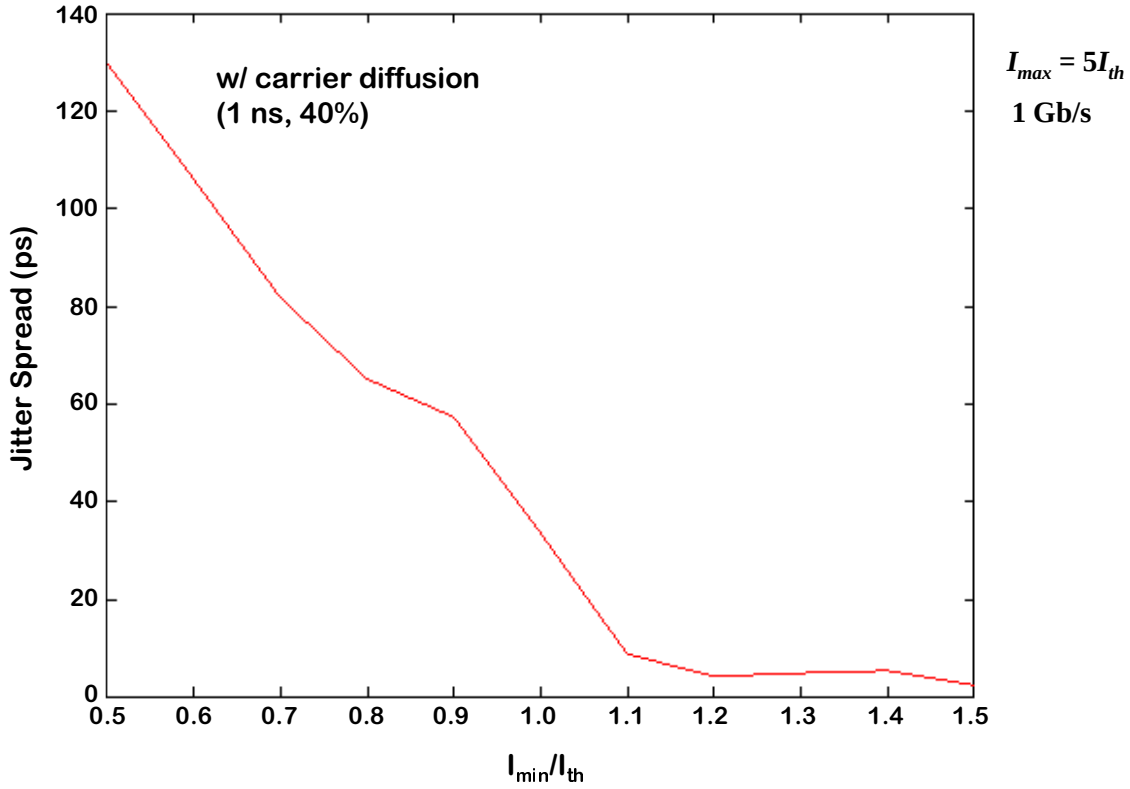
w/ carrier diffusion
(1 ns, 40%)
Jitter Spread (ps)
$I_{min}/I_{th}$
140
120
100
80
60
40
20
0
0.5
0.6
0.7
0.8
0.9
1.0
1.1
1.2
1.3
1.4
1.5
$I_{max} = 5I_{th}$
1 Gb/s

Fig. 4